

Secure and Efficient Federated Learning Through Layering and Sharding Blockchain

Shuo Yuan, *Graduate Student Member, IEEE*, Bin Cao, *Member, IEEE*, Yao Sun, *Member, IEEE*,
and Mugen Peng, *Fellow, IEEE*

Abstract—Federated Learning (FL) has become an essential enabling technology for digital twin in Industrial Internet of Things (IIoT) networks. However, due to the master/slave structure of FL, it is very challenging to resist the single point of failure of the master aggregator and attacks from malicious IIoT devices while guaranteeing model convergence speed and accuracy. Recently, blockchain has been brought into FL systems transforming the paradigm to a decentralized manner thus further improving the system security and learning reliability. Unfortunately, the traditional consensus mechanism and architecture of blockchain systems can hardly handle the large-scale FL task and run on IIoT devices due to the huge resource consumption, limited transaction throughput, and high communication complexity. To address these issues, this paper proposes a two-layer blockchain-driven FL system, called ChainFL, which splits IIoT network into multiple shards as the subchain layer to limit the scale of information exchange, and adopts a Direct Acyclic Graph (DAG)-based mainchain as the mainchain layer to achieve parallel and asynchronous cross-shard validation. Furthermore, FL procedure is customized to deeply integrate with blockchain, and the modified DAG consensus mechanism is proposed to mitigate distortion caused by abnormal models. To provide a proof-of-concept implementation and evaluation, multiple subchains based on Hyperledger Fabric and the self-developed DAG-based mainchain are deployed. The extensive experimental results demonstrated that our proposed ChainFL system outperforms the existing main FL systems in terms of acceptable and fast training efficiency (by up to 14%) and stronger robustness (by up to 3 times).

Index Terms—Federated learning, blockchain, edge computing, digital twin, industrial IoT

I. INTRODUCTION

Digital twin as an emerging technology provides a feasible solution to cope with the dynamic and complex Industrial Internet of Things (IIoT) environment and has been attracting increasing attention from both academia and industry. A digital twin is a logical object constructed in the virtualization space to represent physical objects in the real world in terms of properties, conditions, and behaviors through models and data [2]. In addition, Machine Learning (ML) has been widely acknowledged as an enabling technology to enhance process

awareness, real-time analysis, and state prediction of a digital twin for the physical systems, which in turn optimize the operating of the physical systems. However, to create digital twins mapped physical objects accurately, a large amount of data distributed across a set of devices or places is needed, which faces the “data islands” problem [3]. Integrating data from IIoT devices to the cloud for centralized training and processing not only increases transmission delay and learning convergence time but also brings serious risks of privacy leakage and data abuse.

To tackle these problems, some works bring Federated Learning (FL) into IIoT for digital twin construction to collaborate devices to train a shared ML model in a distributed way while keeping the training data locally [3]–[5]. The biggest benefit getting from FL is that only local models without any raw data need to be shared during the whole learning process [6]. Therefore, the FL method can take full advantage of the resources and data of IIoT devices to implement intelligence endogenous digital twin, such as predictive maintenance of industrial devices, traffic prediction in Internet-of-vehicle networks, and disease diagnosis based on wearable devices. However, some security and efficiency issues of the traditional FL are still exposed to practical applications, which can be summarized as follows.

Security Issues: Traditional FL systems rely on a central aggregator to orchestrate the entire training process. Hence, it is vulnerable to a Single Point of Failure (SPOF) and targeted attacks leading to service paralysis [7]. Moreover, the potential bias of selecting the few same IIoT devices by the central aggregator at each round will damage the accuracy of the global model [8]. In addition, traditional FL cannot detect malicious IIoT devices which do not send the model or even send a wrong model, then heavily disturbing the learning process.

Efficiency Issues: Most FL systems run in a synchronous manner, where the central server waits for all participant IIoT devices to upload local models before updating in each round. Therefore, the convergence speed would inevitably be slowed down by *stragglers* which are devices consuming a prolonged time to complete one training iteration [9]. On the other hand, in asynchronous training, since the model trained from an older version of the global model (called the *stale model*) may be used in the updating, the global model would be unstable.

To address the aforementioned issues, a series of works have introduced blockchain [10], [11] into FL to exploit the advanced features of blockchain, such as tamper-resistant, decentralized, traceability, and so on [12]–[14]. In [12], BlockFL

This work was presented in part at 2021 IEEE WCNC [1].

Shuo Yuan, Bin Cao, and Mugen Peng are with the State Key Laboratory of Networking and Switching Technology, Beijing University of Posts and Telecommunications, Beijing 100876, China (e-mail: yuanshuo@bupt.edu.cn; caobin@bupt.edu.cn; pmg@bupt.edu.cn).

Yao Sun is with James Watt School of Engineering, University of Glasgow, G12 8QQ Glasgow, Scotland, UK. (e-mail: Yao.Sun@glasgow.ac.uk).

This work has been submitted to the IEEE for possible publication. Copyright may be transferred without notice, after which this version may no longer be accessible.

is proposed to carry out synchronous FL training in a decentralized manner. Then, the SPOF and targeted attacks can be overcome, and all local model updates will be verified by blockchain nodes on the Proof-of-Work (PoW) consensus [10]. To alleviate the computation consumption during the consensus, a collaborative system for IIoT is proposed in [13] to integrate the federated training into the consensus process. Besides, some works also introduced differential privacy into blockchain-based FL to further enhance the data privacy of IIoT devices [14]. However, these works have not considered the limitation of blockchain throughput, which is a critical factor in determining the efficiency of the training process.

Although these blockchain-enabled systems have brought some improvements to the distributed training process, the combination of blockchain and FL in IIoT is still challenging.

- 1) *High Computation Cost.* The PoW or PoW-based consensus must present a solution to a computational puzzle to dispute the right of block generation to maintain blockchain stability and security, which brings a huge computation cost [15]. Moreover, the time cost for solving the hash problem ineluctably slows down the convergence of the training task.
- 2) *Limited Scalability.* As we all know, most consensus hardly handles high scalability and decentralization at the same time due to the cost of computation, communication, and time [16]. For example, PoW consensus comes with low transaction throughput due to the intensive hash computation and cannot scale out its transaction processing efficiency with the increase of blockchain nodes. Besides, the throughput of Practical Byzantine Fault Tolerance (PBFT) [17] is limited by the network bandwidth due to the highly frequent communication exchanges.
- 3) *Huge Storage Requirement.* The essence of blockchain is a distributed ledger, and each blockchain node needs to record verified blocks in the local ledger. Therefore, the limited storage of nodes will heavily reduce the speed of information exchange in the network, thereby affecting the delivery of services carried by the blockchain.
- 4) *Stragglers.* Most of the blockchain-enabled FL systems, such as BlockFL [12] and PIRATE [18] are processed in a synchronous manner. Hence, stragglers will retard the efficiency of training, which is similar to the traditional FL. At present, there are few studies on asynchronous training based on blockchain, let alone the detection of stale models [1].

To cope with these challenges, we propose a hierarchical blockchain-driven FL system named ChainFL for scaling and securing decentralized FL. By splitting the large-scale IIoT network into multiple shards, the majority of information exchange and storage is limited in the same shard which significantly reduces the communication rounds and storage requirements. Besides, the model trained from each shard can be obtained and validated by other shards efficiently with the help of the Direct Acyclic Graph (DAG) consensus-based mainchain.

Overall, the main contributions of this paper are summarized as follows: 1) We propose ChainFL, a novel FL system driven

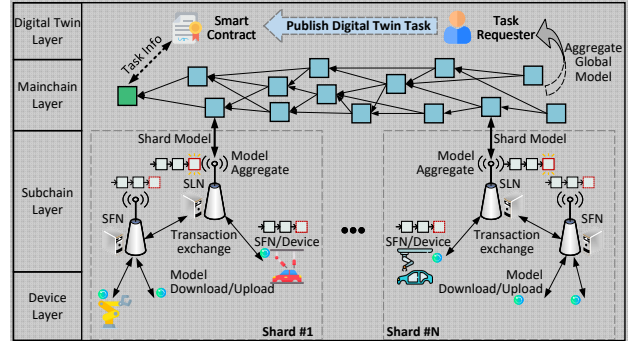


Fig. 1. Layered architecture of ChainFL.

by the hierarchical blockchain, with the aim to provide a secure and effective FL solution for digital twin construction in IIoT networks. We design a Raft-based blockchain sharding architecture to improve scalability and a modified DAG-based mainchain to achieve cross-shard interactions. To the best of our knowledge, ChainFL is the first system using the DAG to coordinate multiple shard blockchain networks to improve the security and scalability of FL systems. 2) We define the operation process and interaction rules for ChainFL to perform the FL tasks. To improve the learning efficiency, synchronous and asynchronous training are combined in ChainFL to alleviate the drag down of stragglers. Moreover, the virtual pruning mechanism is designed based on the modified DAG consensus to eliminate the impact of abnormal models. 3) We establish the sharding network prototype based on Hyperledger Fabric to implement the subchain layer of ChainFL and develop a DAG-based blockchain to implement the mainchain layer of ChainFL as well as fulfill cross-layer interactions. The off-chain storage scheme is adopted in the prototype to reduce the storage requirements of blockchain nodes in both layers. The extensive evaluation results show that ChainFL provides acceptable and sometimes better convergence rates (by up to 14%) compared to FedAvg [6] and AsynFL [19], and enhances the robustness (by up to 3 times) of FL system.

The remainder of this paper is structured as follows. The architecture of ChainFL is introduced in Section II. The details of the ChainFL are presented in Section III, where the workflow and consensus of ChainFL are well described. Afterward, implementation and experimental evaluations are shown in Section IV. This paper is concluded and future works are described in Section V.

II. OUR PROPOSED CHAINFL SYSTEM

As shown in Fig. 1, there are mainly four layers in ChainFL: device layer, subchain layer, mainchain layer, and digital twin layer. The device layer is composed of IIoT devices participating in FL tasks for digital twin construction, such as vehicles, smart machines, and sensors. The subchain layer consists of subchains which are deployed in each shard independently, and responsible for coordinating IIoT devices in the shard to complete the training task in a synchronous manner. The classic multi-access edge computing scenario [20] is considered in the subchain layer, where edge nodes (e.g., IIoT devices and access points with abundant computation resources) are partitioned into multiple independent groups (referred to as

shards) to deploy subchains and act as blockchain nodes to exchange information and establish consensus. To meet the requirements of access control for IIoT devices, the consortium blockchain is adopted in the subchain. Besides, the edge nodes as blockchain nodes in each subchain fall into two categories: Subchain Leader Node (SLN), and Subchain Follower Node (SFN).

The mainchain layer includes a mainchain which adopts the asynchronous consensus mechanism based on DAG architecture (known as DAG consensus [21] or tangle consensus [22]) to handle the interactions with subchains. In the DAG-based mainchain, as shown in Fig. 1, *vertices represent transactions*, and the *edges denote approval of another transaction*. Each transaction in the mainchain network contains one model trained by one shard. The transactions that are not approved by any other transaction are called *tips*. Unlike other blockchain systems, such as PoW-based blockchain, this mainchain does not rely on single chain being the single source of confidence due to the graph structure. The mainchain that can endogenously tolerate forks is able to process the transactions asynchronously. Therefore, ChainFL carried by IIoT networks can be effectively scaled without greatly affecting the system throughput. Finally, the digital twin will be constructed as the mainchain is created and updated as the mainchain grows.

III. CHAINFL WORKFLOW & CONSENSUS

In this section, we start with the blockchained FL algorithm, then detail the FL process and consensus of ChainFL.

A. Blockchained FL Algorithm

As mentioned above, both synchronous and asynchronous training are considered in ChainFL and run in a decentralized manner. Hence, the FL algorithm originally proposed in [6] needs to be modified to adapt to the architecture of ChainFL.

To describe the algorithm clearly, we take shard #1 as an example. We assume that the IIoT device set $\{d_1, d_2, \dots, d_n\}$ is selected by SLN of shard #1 to participate in the FL task, and datasets of these devices are $\{D_1, D_2, \dots, D_n\}$. Without loss of generality, assume that each training sample in dataset is a set of input-output pairs (\mathbf{x}, \mathbf{y}) , where \mathbf{x} is features and \mathbf{y} is the label. The parameters set of the FL model is denoted as \mathbf{w} . For each sample i , the loss function of the machine learning problem is defined as $f_i(\mathbf{w}) = l(\mathbf{x}_i, \mathbf{y}_i | \mathbf{w})$. Therefore, the loss function of device j on the mini-batch b_j , a randomly sampled subset from D_j , can be written as $f_{b_j}(\mathbf{w})$. The goal of device j is to minimize the loss on each mini-batch:

$$\min F_j(\mathbf{w}) = \mathbb{E}_{b_j \sim D_j} f_{b_j}(\mathbf{w}). \quad (1)$$

By applying the gradient descent algorithm on the mini-batch, the local model of device j can be updated according to:

$$\mathbf{w}_j \leftarrow \mathbf{w}_j - \mu_j \nabla f_{b_j}(\mathbf{w}_j), \quad (2)$$

where μ_j is the learning rate of this device. Then, E epochs for local dataset D_j will be executed to train the local model.

In addition, the Federated Averaging algorithm [6] is adopted to aggregate the updated local models uploaded from

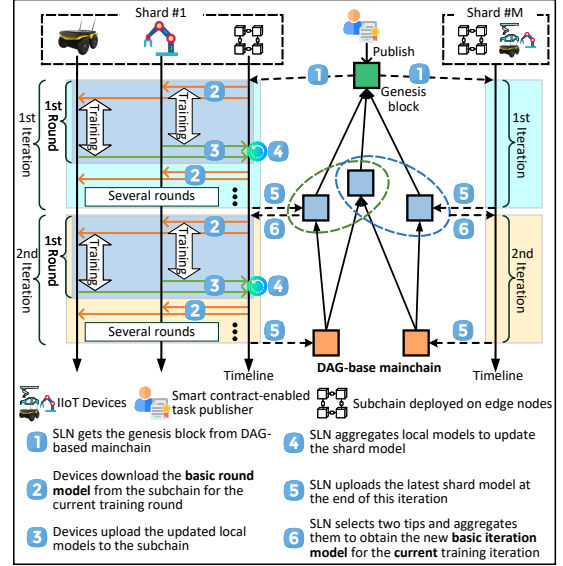


Fig. 2. Overview of the FL process in ChainFL.

the selected devices. Then the loss function of shard #1 on decentralized datasets can be expressed as:

$$G_{s1}(\mathbf{w}) = \sum_{j=1}^m \frac{|D_j|}{D} F_j(\mathbf{w}), \quad (3)$$

where $m(m \leq n)$ is the number of valid models passed the validation during the consensus and $D = \sum_{j=1}^m |D_j|$ is total size of datasets used in this shard training round. As the IIoT devices selected in round k upload the updated local models, the model parameters of shard #1 \mathbf{w}_{s1} is updated through the weighted aggregation of all updated local models' parameters, i.e.,

$$\mathbf{w}_{s1}(k) = \sum_{j=1}^m \frac{|D_j| \mathbf{w}_j(k)}{D}. \quad (4)$$

B. FL Process in ChainFL

To complete the FL task of digital twin in a decentralized manner, we define the operation process and design a set of interaction rules to orchestrate the IIoT devices and edge nodes in ChainFL, as shown in Fig. 2. It is worthy to be noted that there are two kinds of transactions in ChainFL: *subchain transaction* and *mainchain transaction*. The former is created by IIoT devices and SLNs, and spreads within one specific shard. The latter is created by SLNs and spreads in the mainchain network. More details about this procedure are given as follows.

Phase 1: Task Publication. The task requester signs a smart contract to publish an FL task for digital twin construction. The requirements, such as the structure and parameters of the initial model, configurations for shard training, and terminations of this task, will be stated in this contract. Then the smart contract creates the genesis transaction (denoted as g_0) of the mainchain which encapsulates these requirements and a test dataset provided by task requester. Meanwhile, the related shard network(s) will be triggered by this smart contract to perform the training task.

Algorithm 1 ShardTrainingIteration. w_{bim} : basic iteration model, w_{brm} : basic round model, w_s : shard model, R : the number of training round in each iteration.

Each triggered SLN executes:

```

1: obtain  $w_{bim}$  from mainchain for the current shard training iteration
2:  $w_{brm} = w_{bim}$ ,  $w_s = w_{bim}$ ,  $r = 0$ 
3: while  $r < R$  do
4:   encapsulate  $w_{brm}$  and publish to the subchain
5:   select and trigger devices
6:   receive valid local models // waiting devices update
7:    $w_s \leftarrow$  aggregate local models according to (4)
8:    $w_{brm} = w_s$ ,  $r = r + 1$ 
9: end while
10: return  $w_s$ 

```

Nodes in subchain execute:

```

1: receive the transactions from devices
2: for all received transactions do
3:    $A_{new} \leftarrow$  validate the accuracy of the model stored in the transaction
4:   if  $A_{new} > A_\tau$  then
5:     forward the transaction to SLN
6:   else
7:     mark invalid and discard
8:   end if
9: end for

```

Phase 2: Shard Training. g_0 is pulled by SLNs in triggered shard networks. Then the task information parsed from g_0 will be encapsulated into the subchain transaction and stored in the distributed ledger of each shard to initiate the training process. The details of Phase 2 are described as follows:

- *1) Device Selection:* In each training round of one shard, SLN selects candidates for shard training based on the status of IIoT devices such as local data profile and power status reported periodically. Only the devices that are willing to participate in training and have abundant battery and stable network coverage will be selected. Then, these selected devices are authorized to access the subchain to download the basic round model for local training and upload updated local models. It is worth noting that the device selection in each shard is independent.
- *2) Local Update:* Based on the basic round model obtained from the subchain, the device will run the training process over the local raw data to solve problem (1). Then the updated local model will be sent to the subchain node (SLN or SFN) after reaching the goal declared in the smart contract, such as the number of local training epochs or the convergence value of the evaluation metric.
- *3) Model Aggregation:* As shown in Algorithm 1, each subchain node receives local models and validates the accuracy based on the test dataset. The preset threshold A_τ is used to judge the validity of models and could be set as the value of the evaluation metric of the basic round model used in the current training round. Next, SLN will aggregate these valid local models according to (4) to update the *shard model* and then publish it to subchain as the *basic round model* during the shard training iteration. Due to the synchronous manner is used

Algorithm 2 SLN Interact with Mainchain: Basic Iteration Model Building and Shard Model Submitting

```

1: while true do
2:   if the current is 1st iteration then
3:      $w_{bim} \leftarrow$  extract the initial parameters from  $g_0$ 
4:     ApproveSet = ( $g_0$ )
5:   else
6:      $(w'_1, w'_2, \dots, w'_\eta) \leftarrow$  choose  $\eta$  tips from the DAG
7:      $(A'_1, A'_2, \dots, A'_\eta) \leftarrow$  validate the accuracy of the model in each chosen tip
8:      $w_{bim} \leftarrow (\sum_{i=1}^{\lambda} \frac{w'_i}{\lambda})$ , aggregate  $\lambda$  ( $\lambda < \eta$ ) tips with the highest accuracy to build a basic iteration model
9:     ApproveSet = these  $\lambda$  tips
10:   end if
11:    $w_{new} \leftarrow$  ShardTrainingIteration( $w_{bim}$ )
12:    $g \leftarrow$  package  $w_{new}$  and the ID of all transactions in ApproveSet as a mainchain transaction
13:   submit the  $g$  to the mainchain
14:   if stop signal received then
15:     break
16:   end if
17: end while

```

in the shard training, the aggregation of the shard model will be triggered once enough IIoT devices upload local models in time, otherwise the round will be abandoned. The process from device selection to model aggregation is called *a round of shard training*. If the current iteration has not been terminated, the updated shard model will be packed as a subchain transaction and then be published to the subchain to provide the basic round model for the next shard training round.

Phase 3: Shard Model Submitting and Basic Iteration Model Aggregating. When the shard training iteration has been completed, the latest aggregated shard model will be packed as a mainchain transaction and then be submitted to the mainchain by the SLN. Meanwhile, the new *basic iteration model* w_{bim} will be aggregated from the mainchain to start a new shard training iteration if the training task is not over. The details of these processes are shown in Algorithm 2.

In addition, the smart contract will monitor the latest DAG and take similar operations as the basic iteration model aggregation described in Algorithm 2 to aggregate the global model periodically. The number of tips selected to construct the global model is related to the specific task and is stated in the smart contract. The smart contract will send the stop signal to all triggered SLNs while the end condition is met. Then, SLNs will terminate the training process after the current iteration is done. On the other hand, the task requester is also able to aggregate the global model from any location where it can access the mainchain. Besides, IIoT devices licensed to access the edge shard blockchain can select to join the training task to improve the model accuracy or download the latest model to get the latest intelligent service, anytime and anywhere without any centralized management.

C. ChainFL Consensus

The Raft consensus and the DAG consensus are adopted in each subchain and the mainchain, respectively.

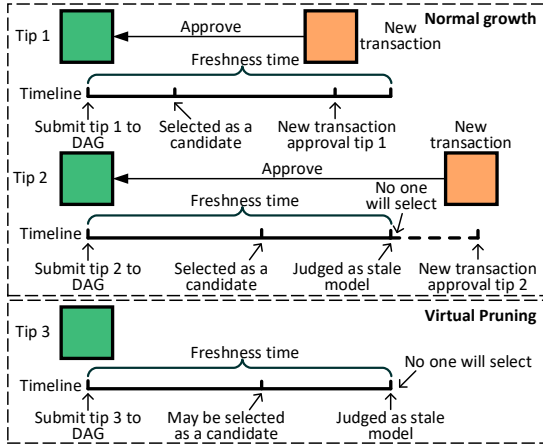


Fig. 3. Three situations in lifecycle of each tip.

1) **Raft Consensus:** The edge nodes in one Raft consensus-based subchain network can be classified into leader and followers. The details of leader selection are not the focus of this paper and can be found in [23]. Since the leader plays a key role in one shard, the ability to deal with problems caused by the leader crash (such as offline or service failure) is very important. Actually, Raft is a distributed Crash Fault-Tolerance (CFT) protocol, which ensures that in the event of crash failure, the subchain network can make decisions and process the training tasks. As the leader crash is detected by a heartbeat mechanism, an election will be proposed by some leader candidates timely. Specifically, the maximum number of failed nodes a in Raft should satisfy $b = 2a + 1$, where b is the total number of edge nodes in one shard. As shown in Algorithm 1, followers are responsible for validating the received transactions (updated local models) and then forwarding the valid ones to the leader. The leader will sort these transactions by the generation time. Once the cumulative size of transactions reaches the threshold or the period ends, the leader will create a block and broadcast it to all followers. The block will be approved by the follower once the signature and transactions in the block are verified. Then, the consensus to this block can be reached when the leader received positive responses from at least half of all followers.

By partitioning a large-scale blockchain network into multiple independent shards, the system throughput is scaled effectively with the help of parallel consensus and separate data storage. In this way, most of the data needs to be synchronized within just one shard instead of the entire network, which considerably reduces communication rounds and speeds up the processing of the transaction confirmation. Moreover, local models will be stored only in the ledger of each shard. The requirements of data storage for blockchain nodes will be reduced significantly. On the other hand, the influence of stragglers can be limited to the shard where stragglers belong instead of the entire network.

2) **DAG Consensus-based Virtual Pruning:** As described in Algorithm 2, SLNs use λ tips to build the basic iteration model. Then, these tips will be approved by the updated shard model (new mainchain transaction) trained from this basic iteration model in the current iteration. However, there are abnormal transactions in the mainchain, which fall into

two types: malicious transactions submitted by malicious shards and stale transactions (transactions that contain the stale model) caused by stragglers. These transactions will be effectively detected by the DAG consensus which combines the voting mechanism with the accuracy validation of main-chain transactions, as presented in Algorithm 2. For instance, transactions with low accuracy have a high probability of being ignored thus cannot be used for the aggregation of the basic iteration model. Compared with normal transactions, abnormal transactions are much less likely to be approved in DAG-based consensus. These unapproved transactions are not dropped but stored as tips in the graph structure of the mainchain. We realize that the proportion of abnormal transactions to all tips increases over time thus, finally increasing the probability that SLNs select abnormal transactions to build the basic iteration model.

To counter this problem, we set a waiting time called *freshness time* in the mainchain to eliminate the effect of abnormal transactions. The freshness time of each tip is independent and starts timing after it is received by the mainchain node. As shown in Fig. 3, each tip experiences one of three situations during the entire lifecycle. The premise for a tip to be approved by other transactions is that at least one SLN selects it as a candidate within the freshness time. The tips that were not selected as candidates for the aggregation of the basic iteration model during the freshness time can no longer be selected. Therefore, the effect of abnormal transactions could be eliminated efficiently with the assistance of the DAG consensus, and then carry out the virtual prune of the DAG. It is noteworthy that although each Raft-based shard can only tolerate crash faults, the impact of shards containing malicious devices and malicious shards on FL tasks can be effectively eliminated in the DAG consensus process.

IV. IMPLEMENTATION AND EXPERIMENTAL EVALUATIONS

In this section, we present the implementation of ChainFL and evaluate the performance of ChainFL in terms of convergence and robustness against model attacks of malicious devices or shards.

A. Implementation

The implementation of ChainFL in real-world environment and the function modules deployed in each entity are shown in Fig. 4(a) and Fig. 4(b), respectively. The details of the practical deployment of ChainFL, which include the off-chain storage scheme, Hyperledger Fabric-based subchain, and modified DAG-based mainchain, are provided in supplementary AppendixV-A. The transaction and block format in ChainFL are presented in Fig. 8 in supplementary AppendixV-A. The implementation of ChainFL is available on GitHub.

B. Baselines and Settings

To evaluate the performance of ChainFL over various models, we run the Convolutional Neural Networks (CNNs)-based realistic object classification as Task 1 and the Gated Recurrent Unit (GRU)-based neural language processing as Task 2 on the

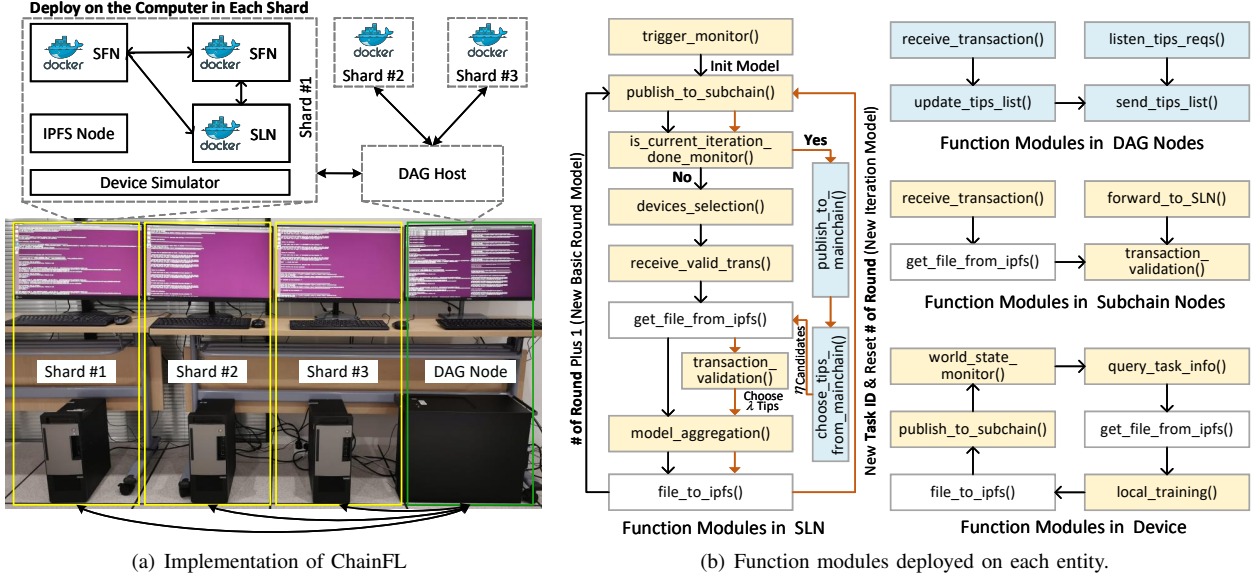


Fig. 4. The implementation of ChainFL in the real environment with the function modules deployed on each entity.

TABLE I
COMMON EXPERIMENTAL SETTINGS.

Parameter	Symbol	Task 1	Task 2
Dataset	D	MNIST	Penn Treebank
Dataset size	$ D $	70000	1036580
Model	w	CNN	GRU
# of devices	n	100	100
Learning rate	μ	$1e-2$	$1e-2$
# of cand. tips	η	3	3
# of appr. tips	λ	2	2
# of shards	M	3	3
Loss function	l	Cross Entropy Loss	NLL Loss
Eval. metric	e_m	$\text{Acc} = \frac{1}{n} \sum_{i=1}^n \phi(y_i, \hat{y}_i)$	$PPL(x) = -\sum_x p(x) \log \frac{1}{p(x)}$
# of dev./shard	S_d	{10, 20, 30}	{10, 20, 30}
Mini-batch size	B	{10, 20, 30, 40, 50}	{10, 20, 30, 40, 50}
Local epochs	E	{1, 5, 10, 15, 20}	{1, 5, 10, 15, 20}
Malicious ratio	M_d	{0, 0.1, 0.2, 0.3}	{0, 0.1, 0.2, 0.3}
# of rounds/ite.	R	{1, 2, 3}	{1, 2, 3}

proposed ChainFL. *Due to space limitation, see supplementary Appendix V-B for the settings and evaluations of Task 2.* The image dataset MNIST [24] is used in Task 1, and the non-IID setting of data is adopted in all experiments. In Task 1, the classic network of LeNet-5 is used as the training model, which consists of two convolutional layers with the max pooling and three fully connected layers. The details of the common experiment settings for these tasks are given in Table I. As shown in the table, we adopt different evaluation metrics (denoted as e_m) for different tasks. For the metric of accuracy (denoted as Acc), the function $\phi(\cdot)$ returns 1 if the output of the model \hat{y}_i matches the label of the sample y , otherwise returns 0.

We conduct extensive experiments for comparisons in multiple dimensions, such as different distributed training methods, the scale of the mini-batch size of local training, and the number of local epochs. There are two baselines in these comparisons, and the settings of baselines and ChainFL are as follows:

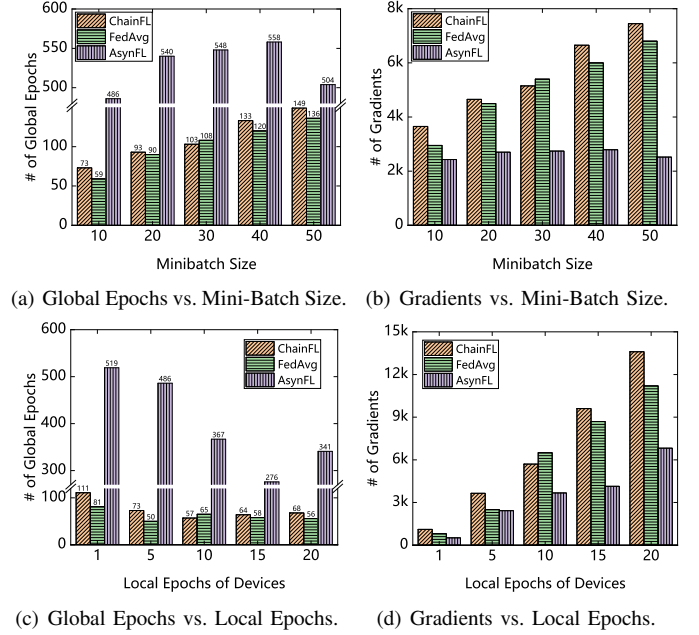


Fig. 5. Effect of the mini-batch size and local epochs of devices on # of global epochs and # of gradients with a preset threshold of the testing accuracy of 0.95 ($S_d = 10$, $R = 1$, $M_d = 0$).

1) *FedAvg* [6]: FedAvg is a synchronous federated optimization method that samples a fraction of devices for each iteration and each device will take several local epochs to update the local model. Besides, the number of sampled devices for each iteration is the same as the number of devices per shard (S_d) for a more fair comparison.

2) *AsynFL* [19]: AsynFL is an asynchronous federated optimization method that updates the global model timely as the central server receives the updated local model from the device. For detail, each updated local model w'_{lm} will be used to update the global model w'_{gm} in each global epoch, and the update rule of the global model is $w'_{new} \leftarrow \frac{1}{2}w'_{gm} + \frac{1}{2}w'_{lm}$.

3) *ChainFL*: The training process in each shard of our proposed ChainFL takes a similar setting with FedAvg and per-

TABLE II
BEST ACCURACY OF TASK 1 UNDER DIFFERENT EXPERIMENTAL SETTINGS OF MINI-BATCH SIZE (B) AND # OF LOCAL EPOCHS (E).

		Best Accuracy									
		Stop@ # of Global Epochs=150					Stop@ # of Gradients=7000				
Mini-Batch Size (B)		10	20	30	40	50	10	20	30	40	50
E=5	FedAvg	0.9702	0.9603	0.9575	0.9552	0.9526	0.9663	0.9602	0.9552	0.954	0.9507
	AsynFL	0.9021	0.8715	0.8511	0.8486	0.8147	0.9759	0.9756	0.9749	0.9724	0.9726
	ChainFL	0.9758	0.9678	0.9683	0.9597	0.9507	0.9756	0.9678	0.9680	0.9545	0.9478
# of Local Epochs (E)		1	5	10	15	20	5	10	15	20	
B=10	FedAvg	0.9632	0.9746	0.9704	0.9715	0.9715	0.9729	0.9619	0.9482	0.9383	
	AsynFL	0.8483	0.9021	0.8774	0.8898	0.8978	0.9759	0.9665	0.959	0.9508	
	ChainFL	0.9701	0.9758	0.9785	0.9780	0.9799	0.97565	0.9625	0.9389	0.8991	

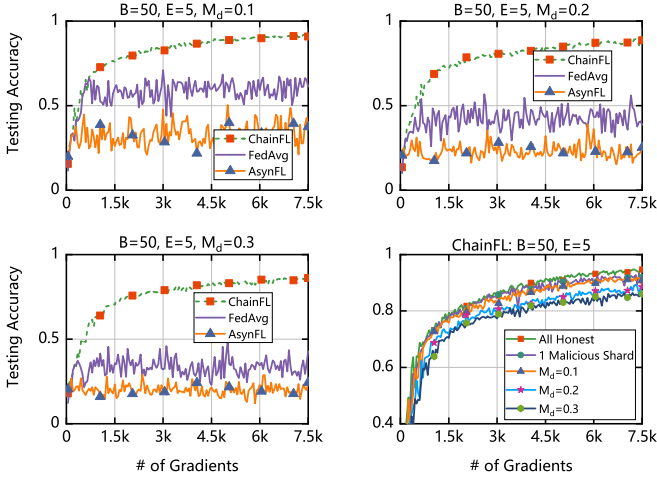


Fig. 6. Effect of different malicious devices ratio on the testing accuracy ($S_d = 10$, $R = 1$).

forms in a decentralized way. Additionally, the basic iteration model for each shard training iteration is independently and asynchronously built from the DAG according to Algorithm 2. There are three shards configured in ChainFL, and S_d devices are non-overlapping selected from the 100 devices for each shard.

Obviously, it is not fair for AsynFL to compare the performance in the scale of the number of global epochs due to the different number of devices selected in each training round. Hence, we conduct two kinds of comparisons: metrics versus the number of global epochs and metrics versus the number of gradients. In fact, the gradient trained in each local epoch of the device can be regarded as the computing power unit. Therefore, the second kind of comparison evaluates the performance on the scale of the same computation cost. For example, the number of gradients used for the global model is 50 when 10 devices are selected in each global epoch and 5 local epochs are performed in each device. For ChainFL, the basic iteration model aggregated from tips by SLN can be regarded as the latest global model of the current DAG due to similar operations with the global model aggregation of the smart contract and the training process in each shard is independent. For these three paradigms, one local epoch of the device local training is a full pass of the local dataset. Furthermore, the communication rounds is not a proper metric to be evaluated in this paper due to the decentralized manner of ChainFL.

C. Experimental Results

First of all, we investigate the sensitivity of the FL model parameters including the size of mini-batch $B \in \{10, 20, 30, 40, 50\}$ and the number of local epochs $E \in \{1, 5, 10, 15, 20\}$. We run training processes with a preset number of global epochs to compare the best accuracy. On the other hand, these training results are recounted as the number of gradients for the second comparison. Besides, we preset the testing accuracy as 0.95. Then, the training process will be terminated when the preset values are reached (higher than 0.95) for the global model. To investigate the model convergence of these three paradigms, we compare the number of global epochs and the number of gradients involved in the training process with preset values. Moreover, we evaluate the robustness of the three training paradigms by configuring multiple malicious devices to attack the accuracy of the global model. Finally, the effect of the number of rounds during one shard training and the number of devices per shard on the global model in ChainFL are investigated.

In task 1 of handwritten digit image classification, we compare the best accuracy achieved in running 150 global epochs and in the training process which produced 7000 gradients. In ‘Stop@ # of Global Epochs = 150’ column of Table II, it is clear that ChainFL is better than FedAvg and AsynFL in terms of global model accuracy in almost all cases with different mini-batch size and local epochs. For instance, ChainFL achieves a roughly 14% improvement of accuracy in the case where $B = 10$ and $E = 1$. The reason is that SLNs in ChainFL build the basic iteration model from the DAG which consisted of models trained from all shards. The superiority of ChainFL in ‘Stop@ # of Gradients = 7000’ column of Table II is reduced compared with AsynFL and maintained compared with FedAvg.

The effects of the mini-batch size and local epochs of devices are also shown in Fig. 5. For details, $E = 5$ in Fig. 5(a) and Fig. 5(b), and $B = 10$ in Fig. 5(c) and Fig. 5(d). To achieve the preset testing accuracy of 0.95, the number of global epochs needed to be executed, and the number of gradients needed to be generated are decreased with the mini-batch size of devices decrease in ChainFL and FedAvg. However, for these three training paradigms, increasing the amount of computation of each device by increasing local epochs will not always reduce the number of global epochs and sometimes reduce the computation efficiency, which concluded from Fig. 5. Besides, in the supplementary Appendix V-B, the testing accuracy of the global model with settings of $B \in \{10, 50\}$ and $E \in \{5, 15\}$ are traced in Fig. 9(a) and

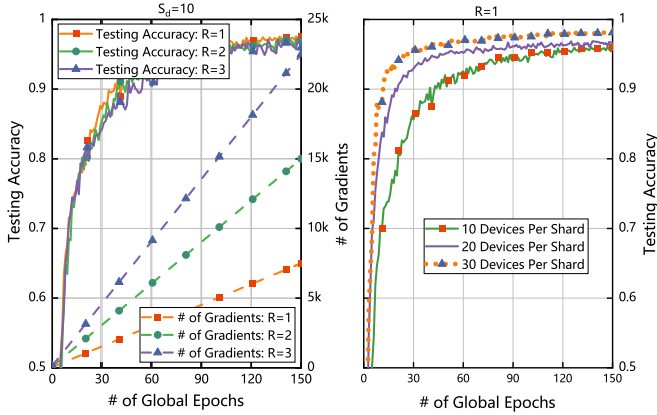


Fig. 7. Effect of rounds per iteration and devices per shard on the testing accuracy ($B = 10$, $E = 5$, $M_d = 0$).

Fig. 9(c), and the corresponding training loss are also given in Fig. 9(b) and Fig. 9(d). From these figures, we can see that ChainFL provides a faster convergence rate and higher accuracy than FedAvg and AsynFL on the number of global epochs scale in most cases.

In addition, another main objective of this paper is to enhance robustness during the training process. Then, we compare the performance of ChainFL, FedAvg, and AsynFL with the different malicious device ratio $M_d \in \{0.1, 0.2, 0.3\}$ (eg. $M_d = 0.1$ means that 10% of all devices in each shard are malicious) in Fig. 6. It is clear that a solid superiority in the model accuracy of ChainFL, especially under the higher malicious ratios $M_d = 0.3$ where 3 times robustness is presented by ChainFL. In the settings of $M_d = 0.2$ and $M_d = 0.3$, the global model accuracy of FedAvg and AsynFL can hardly converge to the value larger than 0.5 in $7.5k$ gradients. But ChainFL converged to the value which is larger than 0.8 in the same settings. Besides, the effects of different malicious levels in ChainFL are also presented in the bottom right corner of Fig. 6. We can observe that the accuracy in ChainFL will decrease slightly with increasing the malicious ratio, which is acceptable compared with the significant drop-down on the accuracy in FedAvg and AsynFL. It is obvious that ChainFL is quite resistant to malicious devices thanks to the consensus on the evaluation metric of the local model in the subchain. Moreover, the consensus-based virtual pruning of the mainchain efficiently eliminate the malicious model published by the malicious shard to maintain a stable convergence of the accuracy of the global model.

We also compare the different ChainFL parameters including the number of rounds $R \in \{1, 2, 3\}$ in one shard training iteration and the number of devices per shard. The results are presented in Fig. 7. We can see that as R increase, the best accuracy of the global model does not increase, which means that more computation costs have not earned equivalent benefits. On the other hand, increasing the number of devices per shard can not only increase the best accuracy but also speed up the convergence of the accuracy of the global model.

V. CONCLUSIONS AND FUTURE WORKS

In this paper, we propose a hierarchical blockchain-driven FL framework ChainFL to improve both efficiency and se-

curity of FL systems for digital twin in IIoT. We adopt the sharding architecture to parallel the consensus among shards to scale the system throughput and then limiting the scale of information exchange and requirements of storage resources. To carry out the consensus on shard models, the cross-layer FL operation procedure and the virtual pruning of the mainchain are designed. Through the shard consensus and DAG-based mainchain consensus, asynchronous and synchronous optimization are effectively combined to deal with the stragglers and stale models. Moreover, the robustness of ChainFL to resist the attack of malicious entities is enhanced with the hierarchical consensus. The prototype of ChainFL is developed and deployed, and massive experiments run in this prototype demonstrated that ChainFL system provides acceptable and sometimes better training efficiency (by up to 14%) and stronger robustness (by up to 3 times) compared with the existing main FL systems.

For future works, the model replacement or double-spending attacks in ChainFL will be analyzed. Moreover, the incentive mechanism based on the blockchain will be investigated to stimulate IIoT devices to participate in FL tasks.

APPENDIX

A. Implementation

The details of the practical deployment of ChainFL, which include the off-chain storage scheme, Hyperledger Fabric-based subchain, and modified DAG-based mainchain, are presented here.

1) *Off-Chain Storage Scheme*: There are two typical categories of blockchain storage scheme: 1) full on-chain storage in which all data is stored in the ledger; 2) off-chain storage in which the data is stored in another file system, and ledger only store a unique identity of the data to guarantee its immutability. Due to the limited block size in Fabric, it is hard to directly store the data stream in the main body of the block. Therefore, the off-chain storage is adopted in the implementation. To store these parameter files, a private peer-to-peer file system called InterPlanetary File System (IPFS) [25] is deployed. As one file is added to IPFS, a hash value that uniquely identifies the contents of this file will be returned. Meanwhile, this hash value can be used to reconstruct the Merkle tree of file pieces of the parameter file and then to download the whole file [25]. Hence, in our implementation, the blockchain only stores the hash value of the parameter file. Furthermore, to upload/download parameter files to/from IPFS during the training process, all IIoT devices and blockchain nodes in ChainFL need to join the IPFS network. The function modules deployed on each entity to interact with IPFS are `file_to_ipfs()` and `get_file_from_ipfs()`, which are presented in Fig. 4(b).

2) *Hyperledger Fabric-based Subchain*: To implement subchains, we set up the Raft blockchain environment based on the Hyperledger Fabric [26] (called Fabric), which includes the Raft ordering consensus. Fabric is a permissioned distributed ledger technology platform, which is suitable for the consortium settings of subchains in ChainFL. With the Public Key Infrastructure (PKI)-based membership management, the Fabric network has plentiful capabilities to control the access

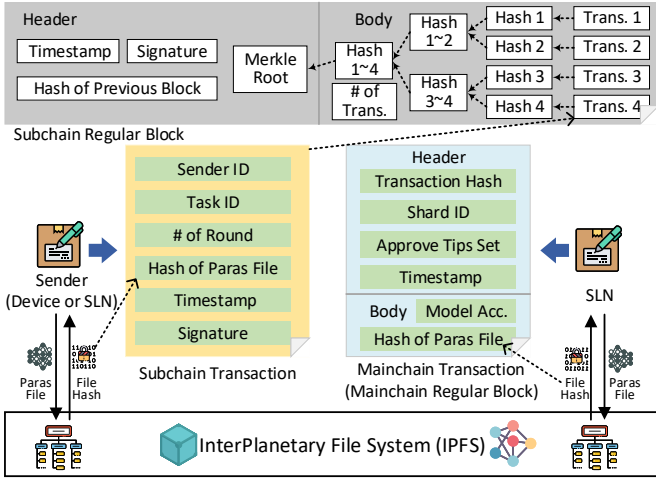


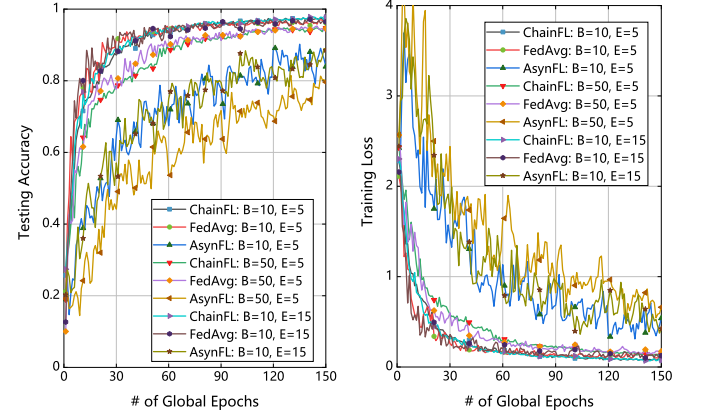
Fig. 8. The format of transactions or/and blocks in ChainFL.

of IIoT devices to carry out the device selection. Besides, a smart contract (called *chaincode*) refined from *sacc* [26] is used to submit transactions to subchains. The information formats of the local model or shard model written to the subchain ledger are shown in Fig. 8. Sender ID in subchain transaction is a unique identifier, which is determined by the identity of transaction issuer and is could be IIoT device ID or SLN ID. Task ID is created by SLN when it starts one *shard training iteration*, and # of Round indicates the index of the current training round in one iteration. Finally, Hash of Paras File is the hash value of one model file in IPFS, and it is the uniform resource identifier to locate the file in IPFS.

The function modules, such as `transaction_validation()` and `model_aggregation()`, which are not original modules of Fabric, are developed and deployed in Fabric nodes to implement the model validation and model/tips aggregation, as shown in Fig. 4(b). Also, the functions related to the interactions with the mainchain, such as `publish_to_mainchain()` and `choose_tips_from_mainchain()`, are deployed and integrated with Fabric nodes. For detail, the scheduling rules and order among these modules are presented in Fig. 4(b). As described in Section III-B, a new basic iteration model should be aggregated from the mainchain when the current iteration is done. The iteration status is indicated by # of Round, for example, the current iteration is done when # of Round reached the number stated in task requirements. Besides, different shard training iteration indicates different Task ID. Then, after constructing the new basic iteration model, SLN needs to create a new Task ID and reset # of Round to start a new shard training iteration.

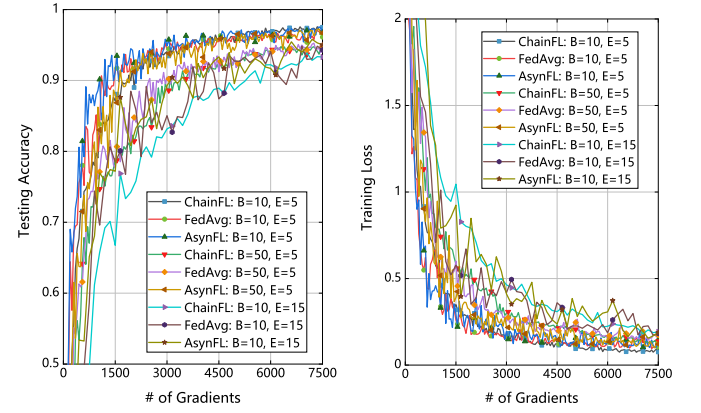
Due to the limited amount of hardware, a complete Fabric-based subchain containing one leader and two followers is configured in one PC¹. In addition, the training process of IIoT devices served by this subchain is also simulated and executed on the same PC. Therefore, the PC and the IIoT devices it served can be regarded as one shard network defined in ChainFL.

¹At least three nodes (one leader and two followers) needed to be deployed in the Raft ordering consensus of Fabric [26].



(a) Accuracy vs. # of Global Epochs.

(b) Loss vs. # of Global Epochs.



(c) Accuracy vs. # of Gradients.

(d) Loss vs. # of Gradients.

Fig. 9. Testing accuracy and training loss of Task 1 on two scales ($S_d = 10$, $R = 1$, $M_d = 0$).

3) *Modified DAG-based Mainchain*: We use Python to develop a modified DAG-based mainchain to exchange the information with shards. The function modules in mainchain nodes are described in Fig. 4(b). The mainchain node maintains a tip list which will be sent to SLNs to response the tips request of SLNs. The request/response between SLN and the mainchain node is implemented by the socket communication. Besides, the tip list will update once SLNs submits a new transaction to the mainchain or the tip is detected as abnormal. The format of transactions in the mainchain is shown in Fig. 8. To accelerate and simplify the executions of massive experiments, the mainchain deployed on one computer (one node) in our real environment setup instead of many distributed nodes².

B. Supplementary Experiences

1) *Supplementary Results for Task 1*: For Task 1, the testing accuracy of the global model with settings of $B \in \{10, 50\}$ and $E \in \{5, 15\}$ are traced in Fig. 9(a) and Fig. 9(c), and the corresponding training loss are also given in Fig. 9(b) and Fig. 9(d).

²Since the interactions between SLNs and the DAG will not be affected by this deployment scheme, the performance of federated learning over ChainFL will not be disturbed.

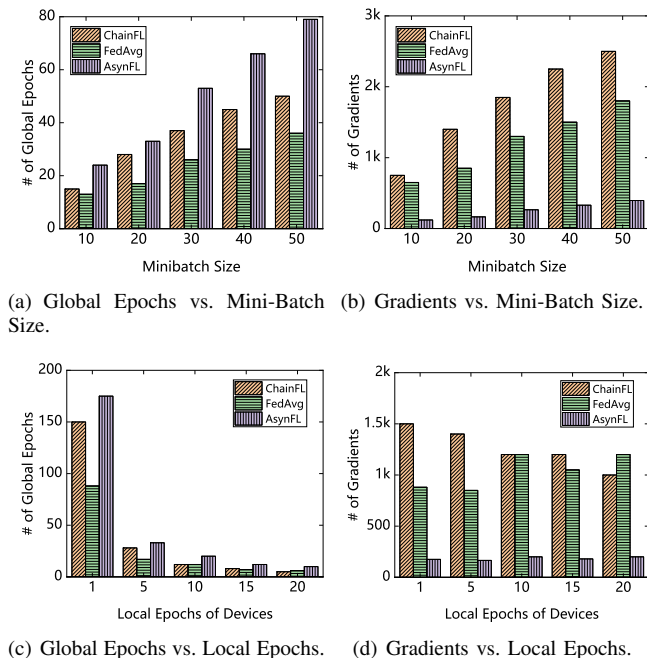


Fig. 10. Effect of the mini-batch size and local epochs of devices on # of global epochs and # of gradients with a preset threshold of the testing perplexity of 150 ($S_d = 10$, $R = 1$, $M_d = 0$).

2) *Settings and Evaluations of Task 2*: To evaluate the performance of ChainFL over various models, we run the Convolutional Neural Networks (CNNs)-based realistic object classification as Task 1 and the Gated Recurrent Unit (GRU)-based neural language processing as Task 2 on the proposed ChainFL. The settings and evaluations of Task 2 are presented as follows. The English language dataset Penn Treebank [27] is used in Task 2. For Task 2, we shuffle the Penn Treebank dataset and random sampling without replacement to split this dataset into 100 subsets allocating to each device respectively. We aim to simulate the real-world scenario of mobile keyboards in decentralized applications. Similar to [28], each text sample is embedded into a 300-dimensions word vector fed to the GRU-based model used in Task 2. Then, the output of the GRU will be fed to the last fully-connected layer to predict the next word. The details of the common experiment settings for these tasks are given in Table I. Perplexity [29] as one of the most commonly metric to measure the quality of language models is used as the metric of Task 2. As shown in Table I, $-\sum_x p(x) \log \frac{1}{p(x)}$ is the entropy of the distribution $p(x)$. The smaller the testing perplexity is, the higher the accuracy achieves and the better the language model trains.

For Task 2, we also ran the training process for a preset number of global epochs and the number of gradients first to observe the best perplexity achieved. As the results are shown in Table III, ChainFL reached a lower perplexity of the global model in most cases, both in the column of ‘Stop@ # of Global Epochs=80’ and ‘Stop@ # of Gradients=3000’. In Fig. 10, we compare the number of global epochs and gradients to reach the specified perplexity of 150 which is the convergence target for the global model. It is clear that these two metrics increase with increasing mini-batch size. Besides, increasing the local epochs to increase the computation parallelism of

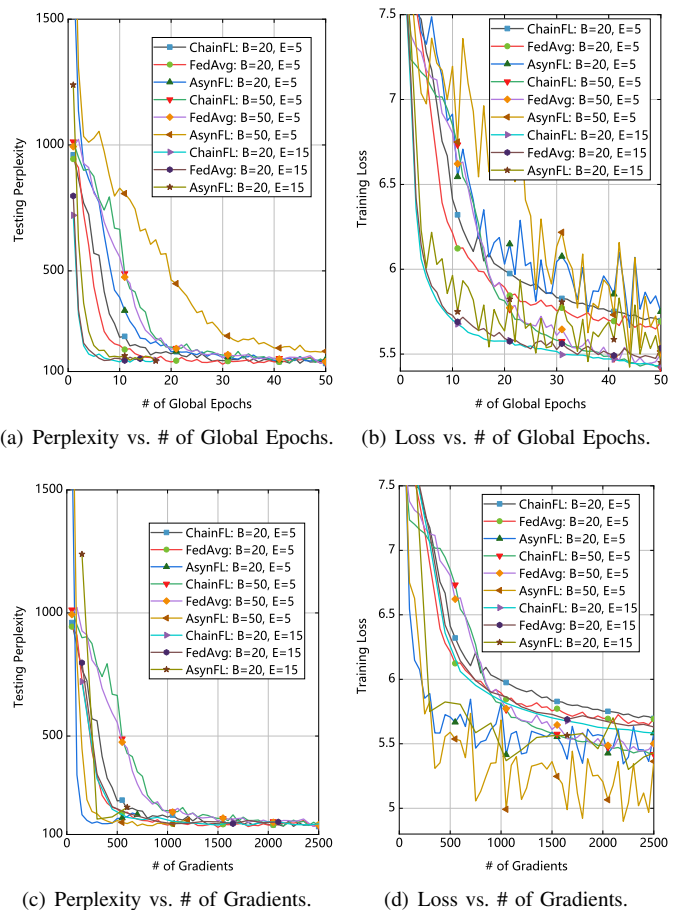


Fig. 11. Testing perplexity and training loss of Task 2 on two scales ($S_d = 10$, $R = 1$, $M_d = 0$).

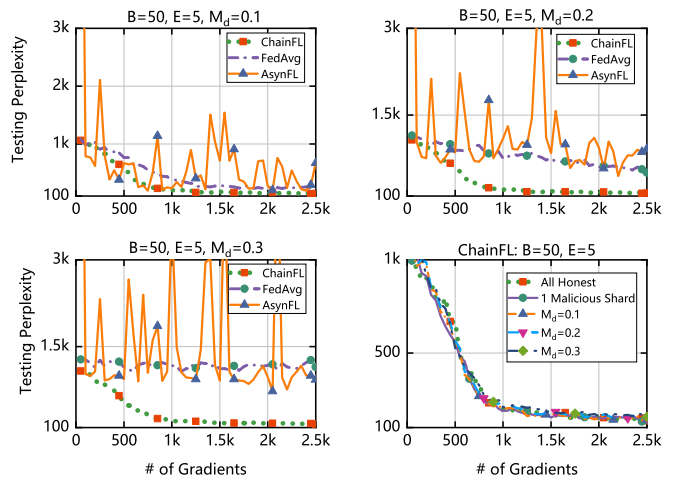


Fig. 12. Effect of different malicious devices ratio on the testing perplexity ($S_d = 10$, $R = 1$).

devices will decrease the number of global epochs. However, the computation costs will not always gain the same benefits, which is shown in Fig. 10(d). Fig. 11 traces the testing perplexity of the global model and the training loss on two scales under the settings of $B \in \{20, 50\}$ and $E \in \{5, 15\}$. We can observe that ChainFL reached a superior performance compared with FedAvg and AsynFL in the setting of $B = 20$, $E = 15$ on the number of global epochs scale. Moreover,

TABLE III
BEST PERPLEXITY OF TASK 2 UNDER DIFFERENT EXPERIMENTAL SETTINGS OF MINI-BATCH SIZE (B) AND # OF LOCAL EPOCHS (E).

		Best Perplexity									
		Stop@ # of Global Epochs=80					Stop@ # of Gradients=3000				
B	E	10	20	30	40	50	10	20	30	40	50
E=5	FedAvg	119.1973	129.0462	128.5419	128.6406	132.7023	119.1973	129.0462	128.5419	128.6406	132.7023
	AsynFL	132.2897	138.1707	137.5729	140.7736	147.04	132.2897	138.1707	135.3072	128.9097	125.5916
	ChainFL	119.302	124.0372	126.8396	129.7998	129.1252	119.302	124.0372	126.8396	134.0198	135.4396
B=10	FedAvg	154.8811	129.0462	133.6719	143.6469	138.19	129.0462	133.6719	143.6469	138.19	
	AsynFL	239.7618	138.1707	141.9482	142.396	149.2502	138.1707	141.9482	142.396	149.2502	
	ChainFL	172.6349	124.0372	131.1227	137.1788	144.9491	124.0372	131.1227	137.1788	144.9491	

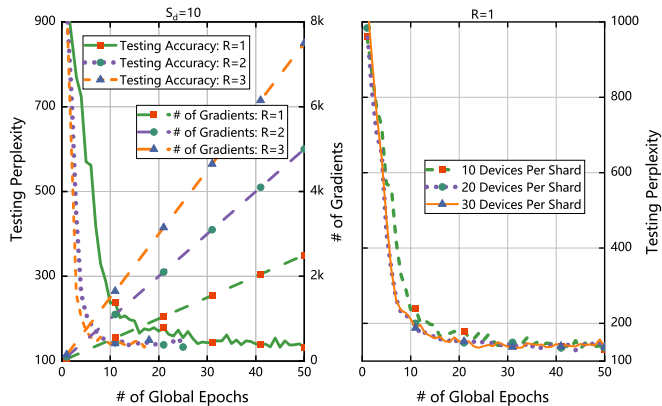


Fig. 13. Effect of rounds per iteration and devices per shard on the testing perplexity ($B = 20$, $R = 5$, $M_d = 0$).

the convergence and perplexity of ChainFL also outperform FedAvg on the number of gradients scale.

The resistance for malicious devices also evaluated in Task 2 and the results are shown in Fig. 12. It can be observed that the testing perplexity of ChainFL more stable than FedAvg and AsynFL. The larger the malicious ratio the more chaos and the larger perplexity of FedAvg and AsynFL. Besides, we can clearly see that the robustness of ChainFL to handle the malicious attacks in the fourth subfigure in Fig. 12. On the other hand, the effect of the number of rounds $R \in \{1, 2, 3\}$ in one shard training iteration and the number of devices per shard $S_d \in \{10, 20, 30\}$ are also investigated in Task 2. As shown in Fig. 13, the testing perplexity of the global model will be decreased slightly by increasing R and S_d .

By conducting massive experiments on Task 1 and Task 2, we can observe some interesting results. In terms of sensitivity of FL parameters, such as B and E , ChainFL has the same characters as FedAvg. With the increase of computation per device, the convergence will be speeded when the local training has not taken full advantage of the local data. However, a larger E will lead to overfitting when the local data has been fully utilized, which will negatively affect the global model. From Fig. 5 for Task 1 and Fig. 10 for Task 2, we can observe that ChainFL needs more global epochs and gradients to reach the preset values (accuracy/perplexity of 0.95/150). Although ChainFL is slightly worse than FedAvg due to the model consensus among multiple shards in the early stage, the training process of ChainFL in the later stage usually brings faster convergence and higher accuracy with the assistance of other shards, which are indicated in Fig. 9 and Fig. 11.

Besides, in an environment where there are no malicious devices and stale models are not considered, the AsynFL can perform fast and stable iterative updates to achieve better performance, which is in line with the conclusions of [19]. However, the performance of AsynFL will suffer a significant decrease while malicious devices exist and show no resistance to attacks. We can observe that ChainFL is quite resistant to malicious devices thanks to the consensus on the evaluation metric of the local model in the subchain. Moreover, the consensus-based virtual pruning of the mainchain efficiently eliminate the malicious model published by the malicious shard to maintain a stable convergence of the accuracy of the global model.

REFERENCES

- [1] S. Yuan, B. Cao, M. Peng, and Y. Sun, "ChainsFL: Blockchain-driven federated learning from design to realization," in *Proc. IEEE Wireless Commun. Networking Conf., WCNC'21*. Nanjing, China: IEEE, Mar. 2021, pp. 1–6.
- [2] R. Minerva, G. M. Lee, and N. Crespi, "Digital twin in the IoT context: A survey on technical features, scenarios, and architectural models," *Proc. IEEE*, vol. 108, no. 10, pp. 1785–1824, Oct. 2020.
- [3] W. Sun, S. Lei, L. Wang, Z. Liu, and Y. Zhang, "Adaptive federated learning and digital twin for industrial internet of things," *IEEE Trans. Ind. Inf.*, vol. 17, no. 8, pp. 5605–5614, Aug. 2021.
- [4] Y. Lu, X. Huang, K. Zhang, S. Maharjan, and Y. Zhang, "Communication-efficient federated learning for digital twin edge networks in industrial IoT," *IEEE Trans. Ind. Inf.*, vol. 17, no. 8, pp. 5709–5718, Aug. 2021.
- [5] Y. Lu, S. Maharjan, and Y. Zhang, "Adaptive edge association for wireless digital twin networks in 6G," *IEEE Internet Things J.*, vol. 8, no. 22, pp. 16219–16230, Jul. 2021.
- [6] B. McMahan, E. Moore, D. Ramage, S. Hampson, and B. A. y Arcas, "Communication-efficient learning of deep networks from decentralized data," in *Proc. Int. Conf. Artif. Intell. Stat., AISTATS'17*, Fort Lauderdale, Florida, USA, Apr. 2017, pp. 1273–1282.
- [7] M. Cao, L. Zhang, and B. Cao, "Toward on-device federated learning: A direct acyclic graph-based blockchain approach," *IEEE Trans. Neural Netw. Learning Syst.*, pp. 1–15, 2021.
- [8] E. Bagdasaryan, A. Veit, Y. Hua, D. Estrin, and V. Shmatikov, "How to backdoor federated learning," in *Proc. Int. Conf. Artif. Intell. Stat., AISTATS'20*, Jun. 2020, pp. 2938–2948.
- [9] S. Dutta, G. Joshi, S. Ghosh, P. Dube, and P. Nagpurkar, "Slow and stale gradients can win the race: Error-runtime trade-offs in distributed SGD," in *Proc. Int. Conf. Artif. Intell. Stat., AISTATS'18*, Playa Blanca, Lanzarote, Canary Islands, Spain, Aug. 2018.
- [10] S. Nakamoto, "Bitcoin: A peer-to-peer electronic cash system," pp. 1–9, 2008. [Online]. Available: <https://bitcoin.org>
- [11] Y. Lu, X. Huang, K. Zhang, S. Maharjan, and Y. Zhang, "Low-latency federated learning and blockchain for edge association in digital twin empowered 6G networks," *IEEE Trans. Ind. Inf.*, vol. 17, no. 7, pp. 5098–5107, Jul. 2021.
- [12] H. Kim, J. Park, M. Bennis, and S.-L. Kim, "Blockchain on-device federated learning," *IEEE Commun. Lett.*, vol. 24, no. 6, pp. 1279–1283, Jun. 2020.

- [13] Y. Lu, X. Huang, Y. Dai, S. Maharjan, and Y. Zhang, "Blockchain and federated learning for privacy-preserved data sharing in industrial IoT," *IEEE Trans. Ind. Inf.*, vol. 16, no. 6, pp. 4177–4186, Jun. 2020.
- [14] L. Cui, Y. Qu, G. Xie, D. Zeng, R. Li, S. Shen *et al.*, "Security and privacy-enhanced federated learning for anomaly detection in IoT infrastructures," *IEEE Trans. Ind. Inf.*, vol. 18, no. 5, pp. 3492–3500, May 2022.
- [15] Q. Yang, Y. Zhao, H. Huang, Z. Xiong, J. Kang, and Z. Zheng, "Fusing blockchain and AI with metaverse: A survey," *arXiv preprint arXiv:2201.03201*, pp. 1–17, Jun. 2022.
- [16] K. Croman, C. Decker, I. Eyal, A. E. Gencer, A. Juels, A. Kosba *et al.*, "On scaling decentralized blockchains," in *Proc. Financial Cryptogr. Data Secur., FC'16*, Christ Church, Barbados, 2016, pp. 106–125.
- [17] M. Castro and B. Liskov, "Practical byzantine fault tolerance," in *Proc. Symp. Oper. Syst. Des. Implement., OSDI'99*, New Orleans, USA, Feb. 1999, pp. 1–14.
- [18] S. Zhou, H. Huang, W. Chen, P. Zhou, Z. Zheng, and S. Guo, "PIRATE: A blockchain-based secure framework of distributed machine learning in 5G networks," *IEEE Netw.*, vol. 34, no. 6, pp. 84–91, Nov. 2020.
- [19] C. Xie, S. Koyejo, and I. Gupta, "Asynchronous federated optimization," *arXiv preprint arXiv:1903.03934*, Sep. 2019.
- [20] W. Sun, J. Liu, Y. Yue, and P. Wang, "Joint resource allocation and incentive design for blockchain-based mobile edge computing," *IEEE Trans. Wireless Commun.*, vol. 19, no. 9, pp. 6050–6064, Sep. 2020.
- [21] Y. Li, B. Cao, M. Peng, L. Zhang, L. Zhang, D. Feng *et al.*, "Direct acyclic graph-based ledger for internet of things: Performance and security analysis," *IEEE/ACM Trans. Networking*, vol. 28, no. 4, pp. 1643–1656, Aug. 2020.
- [22] S. Popov, "The tangle," IOTA, White Paper, Apr. 2018.
- [23] D. Ongaro and J. Ousterhout, "In search of an understandable consensus algorithm," in *Proc. USENIX Annu. Tech. Conf., USENIX ATC'14*, Philadelphia, PA, USA, 2014, pp. 305–319.
- [24] Y. LeCun, L. Bottou, Y. Bengio, and P. Haffner, "Gradient-based learning applied to document recognition," *Proc. IEEE*, vol. 86, no. 11, pp. 2278–2324, Nov. 1998.
- [25] J. Benet, "IPFS - content addressed, versioned, P2P file system," *arXiv preprint arXiv:1407.3561*, pp. 1–11, Jul. 2014.
- [26] "Hyperledger fabric." [Online]. Available: <https://github.com/hyperledger/fabric>
- [27] M. Marcus, B. Santorini, and M. A. Marcinkiewicz, "Building a large annotated corpus of english: The penn treebank," *Sch. Commons*, Oct. 1993.
- [28] S. Ji, S. Pan, G. Long, X. Li, J. Jiang, and Z. Huang, "Learning private neural language modeling with attentive aggregation," in *Proc. Int. Jt. Conf. Neural. Networks., IJCNN'19*, Budapest, Hungary, Jul. 2019, pp. 1–8.
- [29] T. Mikolov, S. Kombrink, L. Burget, J. Černocký, and S. Khudanpur, "Extensions of recurrent neural network language model," in *Proc. IEEE Int. Conf. Acoust. Speech Signal Process, ICASSP'11*, 2011, pp. 5528–5531.